Volume 9, Number 11
1009-1963/2000/09(11)/0827-06
CHINESE PHYSICS
November, 2000
© 2000 Chin. Phys. Soc.

LASING FROM A DYE-DOPED PENDANT DROP AND ITS PRECESSION

Pu Xiao-yun(普小云)[a)b)] and Lee Wing-Kee(李荣基)[b)]
[a)] *Department of Physics, Yunnan University, Kunming 650091, China*
[b)] *Department of Physics, The Chinese University of Hong Kong, Shatin, Hong Kong, China*

(Received 24 March 2000; revised manuscript received 7 July 2000)

We have observed lasing from the rim of dye-doped ethylene glycol pendant drops. Spatial-resolved spectral measurements show that the lasing wavelength varies along a vertical rim of the drop. Time-resolved measurements indicate that lasing precession occurs within the drop. Various lasing patterns due to lasing precession are explained. The measured precession periods for different pumping points are in good agreement with the calculated values based on morphology-dependent resonance theory.

Keywords: pendant drop, lasing precession, red shift
PACC: 4255M, 4260D

I. INTRODUCTION

Pendant drops have been used for measuring liquid surface tension[1], investigating high order-rainbows[2] and studying chemical lasing.[3] Due to the mismatch of refractive index at liquid-air interface, a light ray impinging on the inner surface of a pendant drop, at an incident angle greater than the critical angle, can be trapped for a long time in the drop by total internal reflections. A pendant drop whose shape is not totally symmetric forms a unique optical cavity that may lead to interesting applications.

Properties of lasing in microdroplets of size from 10 to 100μm have been experimentally studied by Tzeng *et al.*[4] For a spherical cavity, lasing was observed from a sample of CaF_2:Sm^{++} of 2 mm diameter.[5] Stimulated emission into optical whispering gallery modes (or morphology-dependent resonances, MDRs) was used to interpret the observed lasing phenomena. MDRs were also observed in the elastic back scattering light from fibre-supported water pendant drops of diameter between 0.6 and 1.5mm.[6] The authors of Ref.[3] suggested that the observed chemical lasing was supported by MDRs.

MDRs of a dielectric sphere are described by a radial mode index l, an angular momentum index n, and an azimuth mode number m of values $\pm n, \pm(n-1), \cdots, 0$. A MDR occurs when $\chi_{n,l} = 2\pi a/\lambda_{n,l}$,[7] where $\chi_{n,l}$ is the Mie size parameter, a and $\lambda_{n,l}$ are the radius of the sphere and the wavelength of light in vacuum, respectively. MDRs within the lasing gain profile may provide large enough optical feedback necessary for lasing. For a spherical cavity, the spatial distribution of an m-mode MDR is confined to a great circle along the rim of the sphere. The light wave supported by this m-mode MDR traces out the same great circle as its orbit. Due to the fact that all m-mode MDRs have the same perimeter length, they are spectrally $(2n+1)$-fold degenerate. However, if the sphere is slightly distorted to become a spheroid, each great circle, except that in the equatorial plane, becomes a great ellipse along the rim of the spheroid. The great ellipse for each m has a different perimeter. Theories[8,9] and experiments[10] have shown that the $(2n+1)$-fold degenerate MDRs of the spherical droplet are frequency shifted and become $(n+1)$ spectrally distinct MDRs. The trace of a light ray does not form a closed curve after one round trip, but precesses along the rim of the spheroid and forms a so-called precession orbit. In terms of MDR, the normal to the m-mode plane that is a great ellipse rotates about the symmetric axis of the spheroid at a fixed tilting angle. This phenomenon was first observed in stimulated Raman scattering (SRS) in nonspherical microdroplets by Swindal *et al.*[11]

A pendant drop, whose shape can be continuously varied, provides an ideal system for the investigation of asymmetric resonant cavities (ARCs).[12] For an axisymmetric pendant drop of size much larger than those of microdroplets and its shape significantly different from a spheroid, new features of lasing are expected to appear. A better understanding of the optical properties of a pendant is therefore essentially for the studies of ARCs, which is the main motivation for carrying out this investigation.

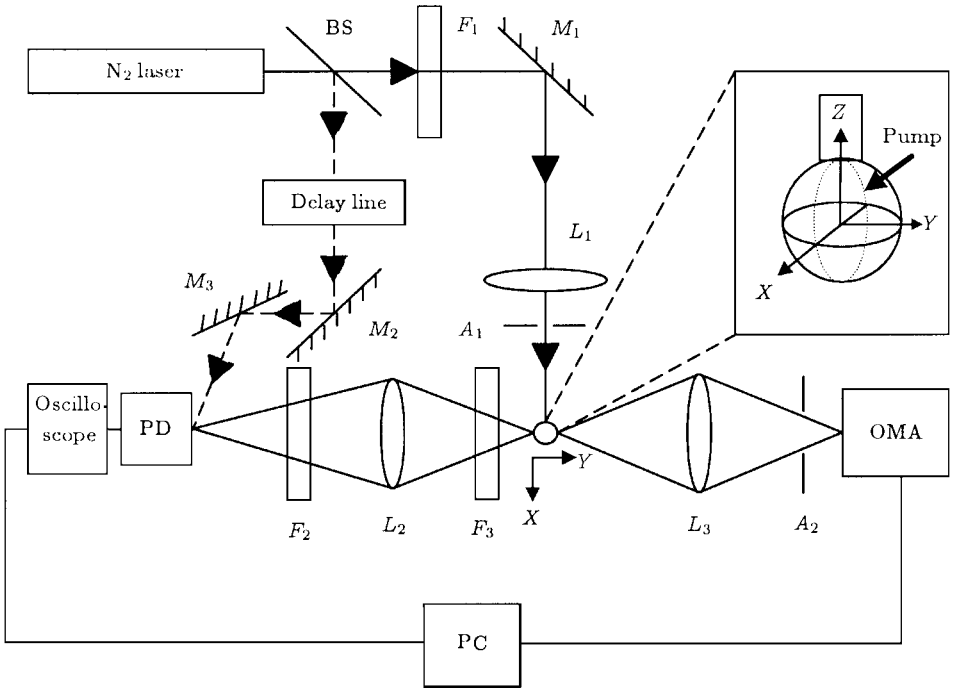


Fig.1. Experimental set-up. F_1, F_2, and F_3: variable, neutral density, and colour filters, respectively; L_1, L_2, L_3—lenses; M_1, M_2, M_3—mirrors; A_1, A_2—apertures; PD—photodiode; PC—microcomputer. For capturing the images of lasing pattern, PD and oscilloscope were replaced by a CCD camera.

II. EXPERIMENT SETUP

In our experiment, R6G dye was dissolved in ethylene glycol with a concentration C=4.2×10^{-3}M. As shown in Fig.1, a syringe was used to suspend a dye solution pendant drop of dimensions 2.7 and 3.2 mm in the equatorial and vertical directions, respectively. A nitrogen laser beam (pulse duration 800ps, wavelength 337nm) was focused to a spot size of ~0.2 mm, and illuminated parallel to X direction at different positions of the pendant drop as depicted in the bottom right corner of Fig.2. Image of the pendant drop was formed onto a CCD camera (SBIG, ST-8) of 1530×1020 elements located along the negative Y direction and recorded by a PC. In front of the CCD camera, a colour filter was used to block scattered nitrogen laser light and a neutral filter of OD=4.05 was used to prevent the CCD camera from saturation. In the Y direction, an optical multichannel analyzer (OMA) with a grating of 1350 grooves/mm was used to obtain the spectra of lasing and fluorescence from the pendant drop. An aperture just in front of the entrance slit of the OMA, together with an imaging lens was used to select a certain portion of the pendant drop image onto the slit. A variable neutral density filter was used to attenuate the nitrogen laser beam, so that the dependence of light intensities from selected portions of the image on pump energy could be investigated.

For time-resolved measurements, the CCD camera was replaced by a photodiode (NEWFOCUS, 25-GHz) to detect two light beams. One from a selected portion of the pendant drop, while the other a time delayed reference light–a 5.2 ns time delayed nitrogen laser pulse relative to the pump. The two beams spatially overlapped on the active area of the photodiode. A fast digitising oscilloscope (TEKTRONIX-520C, 500 MHz) was used to record signals from the detector. By comparing the time difference between the lasing and the reference pulses, the period of lasing precession was deduced.

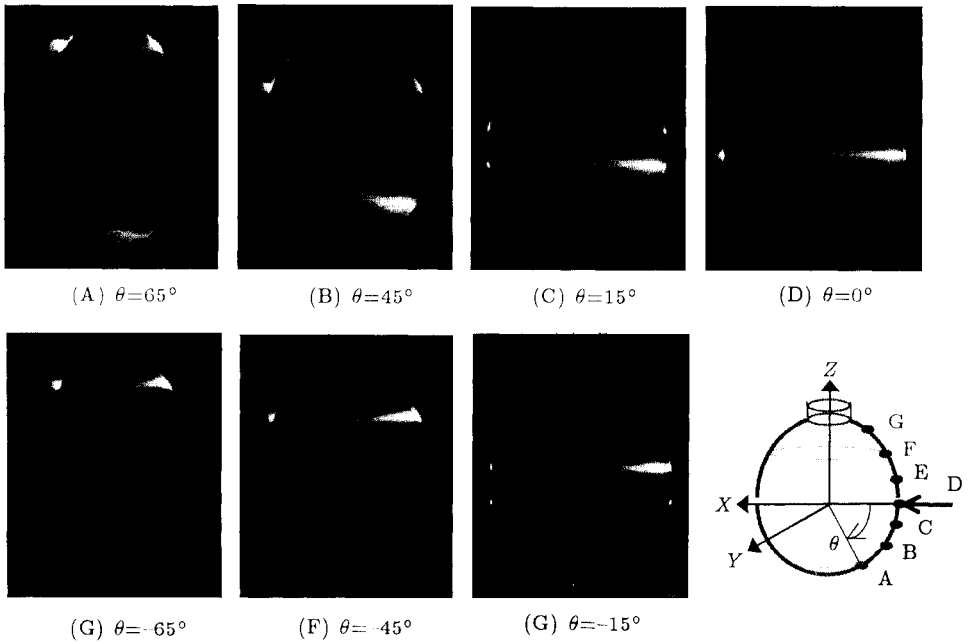


Fig.2. Images of lasing pattern for different pumping points. The drawing in the bottom right corner indicates the pumping points..

Ⅲ. RESULTS AND DISCUSSION

A. Lasing wavelength dispersion along the vertical rim

When the pump beam, parallel to the X-axis, illuminated a pendant drop at different pumping points A–G as shown in Fig.2, one or two pairs of bright spots appeared on the rim of the pendant drop, and fluorescence basically occurred along the pump beam. The positions of the bright spots were found to be cylindrically symmetric to the Z-axis which was the symmetric axis of the pendant drop. The light beams from the bright spots were found to emit almost tangentially from the rim. Spectrally integrated emission intensity from the fluorescent region exhibited a linear dependence on the pump energy from 0.001 to 0.3 mJ. Let θ be the angle between the equatorial plane and the line connecting the pumping point and the origin, as shown in the bottom right corner of Fig.2. The intensities from the bright spots within the equatorial plane (θ=0°) also exhibited a linear dependence on the pump energy below 0.02 mJ. Beyond this value, like most lasers, the intensities exhibited a rapid non-linear increase as the pump energy was increased. The value 0.02 mJ was taken to be the lasing threshold $E_{\rm th}(\theta = 0°)$. $E_{\rm th}(\theta)$ increased as the pumping point was progressively moved away from the equatorial plane: $E_\theta(\theta = 30°)$=0.054 mJ and $E_{\rm th}(\theta = 60°)$=0.061 mJ, this behaviour will be explained at the end of Section ⅢB.

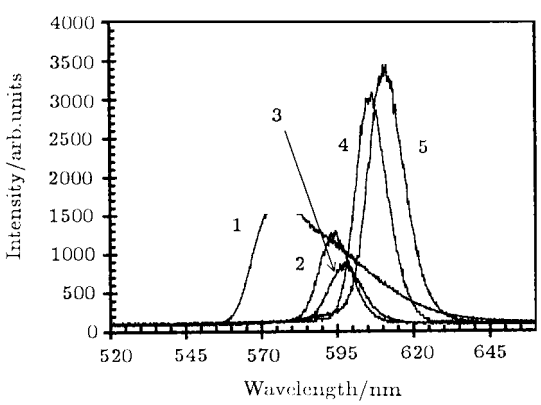


Fig.3. Fluorescent spectra (1) and lasing spectra from different pumping points (2: $\theta = 0°$, 3: $\theta = 25°$, 4: $\theta = 45°$, and 5: $\theta = 65°$), C=4.2×10^{-3}M.

The fluorescent spectrum shown in Fig.3 shows a broad spectral width and peaks at $\lambda = 575$ nm. On the other hand, for a fixed pumping position, all lasing spots have essentially the same spectrum of a much narrower spectral width. When the pumping point was moved from the equatorial plane towards the bottom of the pendant drop ($\theta = 90°$), both the spectral width and the wavelenght of the lasing spots increased, as shown in Table 1. This phenomenon of lasing wavelength red shift along the vertical rim may

be explained by several ways, we will compare it with the theoretical results based on m-mode splitting of MDRs.[8,9] For a slightly distorted sphere (prolate) of polar radius $r_{\rm p}$ and equatorial radius $r_{\rm e}$ Ref.[8] gives the frequencies for the m-mode MDRs of a given n as follows,

$$\omega(m) = \omega_{\rm o}\left\{1 - \frac{e}{6}\left[1 - \frac{3m^2}{n(n+1)}\right]\right\}, \qquad (1)$$

where $\omega_{\rm o}$ is the frequency of the degenerate MDRs of a sphere. The degree of deviation from a sphere is called distortion defined as $e = (r_{\rm p} - r_{\rm e})/a$, where a is the radius of a sphere of the same volume as the prolate spheroid. Equation(1) is valid for $e \ll 1$. Substituting $m = n\cos\theta$ into Eq.(1), we get the wavelength ratio as follows,

$$\frac{\lambda(\theta)}{\lambda(\theta = 0^\circ)} = \frac{\left(1 + \frac{e}{3}\right)}{\left(1 - \frac{e}{6} + \frac{e}{2}\cos^2\theta\right)}, \qquad (2)$$

meaning that $\lambda(\theta)$ increases with θ, and reaches a maximum at the pole of the prolate spheroid ($\theta = 90^\circ$), which is in qualitative agreement with our experimental finding. Fitting the spectral data listed in Table 1 with Eq.(2), we get a fitting parameter value $e = 0.070 \pm 0.005$. Since the shape of a pendant drop deviated slightly from a prolate spheroid, we denote the parameter by $e_{\rm eff}$ and call it effective distortion of the pendant drop.

Table 1. Lasing wavelength and width as functions of θ. λ is the wavelength at the peak of the lasing spectrum; $\Delta\lambda$ is the lasing spectral width (FWHM).

$\theta/(^\circ)$	0	25	45	60
λ/nm	594±1	597±1	605±1	611±1
$\Delta\lambda$/nm	14±1	15±1	15±1	16±1

For a spherical droplet, the frequency spacing between two MDRs of the same order and mode numbers differ by one is $\sim c/2\pi r_{\rm e} m_{\rm r}$,[7] where $m_{\rm r}$ is the refractive index of the drop and c is the speed of light in vacuum. As the size of the pendant drop is $\sim$ 2mm, the wavelength spacing is $\sim$ 0.02 nm, which is too small to be resolved by our OMA. The broad lasing spectrum is likely the stimulated emission supported by many unresolved MDRs.

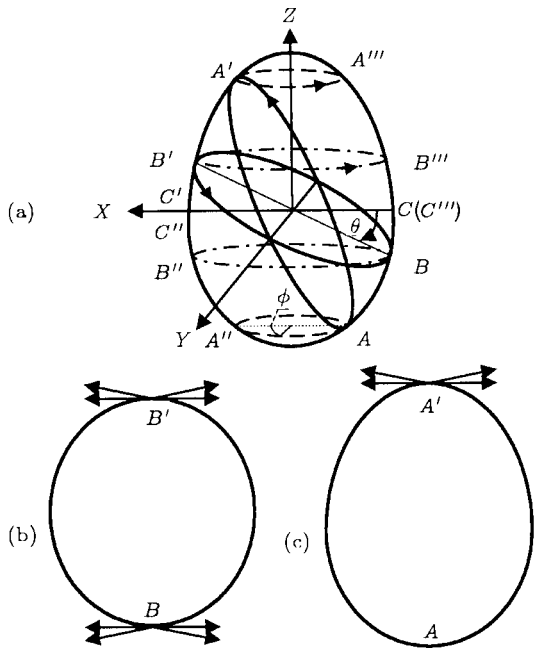


Fig.4. Diagram for illustrating lasing precession (a). A slightly distorted "great ellipse" passing through BB' (b), and a greatly distorted "great ellipse" passing through AA' (c). Arrows in (b) and (c) indicate the laser output.

B. Lasing precession

If we approximate a pendant drop by a prolate spheroid, lasing will then be supported by MDR modes $m = \pm n\cos\theta$ when the pump laser pulse illuminates position B of the pendant drop, as shown in Fig.4(a). If the drop were a sphere, only two lasing spots located at B ($m = -n\cos\theta$) and $B'(m = n\cos\theta)$ would have been observed along the $\pm Y$ directions. For a pendant drop, due to precession, the lasing spots observed at B and B' will precess to B'' and B''' after half a precession period. Since the precession period was of the order of 10^{-9} s and the exposure time of the CCD camera was $\sim 10^{-2}$ s, four lasing spots were recorded. From a geometric optics viewpoint, a light ray starting from A does not end at A after a round trip along the rim of the pendant drop. The end point is shifted from A by a small angle $\Delta\phi$ (decreases when θ increases). After many round trips such that the summation of $\Delta\phi$ is essentially π, point A precesses to point A'' and one half the precession period is completed. Let $t_{\rm P}$ be the time difference between the time-delayed reference pulse and the lasing signals, $\tau_{\rm P}$ be the precession period, where the subscript P indicates the position of the lasing spot. According to the above picture, $t_{A'''}$, $t_{B'''}$, $t_{C'''}$, should be different and $\tau_{\rm P}$ can be determined by $t_{\rm P'''} - t_{\rm P'} = \tau_{\rm P}/2$. The lower part of a pendant drop was

pumped at different positions with the pump beam parallel to the X-axis. Lasing from three positions $A'''(\theta = 60°)$, $B'''(\theta = 30°)$, $C'''(\theta = 0°)$, together with the time-delayed reference pulses are shown in Fig.5, which shows $t_{C'''} > t_{B'''} > t_{A'''}$. This result supports the precession picture. The precession periods are $\tau_A = 0.96 \pm 0.02$ ns, $\tau_B = 0.64 \pm 0.02$ ns and there is no detectable difference between $t_{C'''}$ and $t_{C'}$. Based on the theoretic result of Ref.[8], Swindal *et al.*[11] found the following formula of the precession frequency for a prolate spheroid,

$$\Omega \approx \frac{\mathrm{d}\omega(m)}{\mathrm{d}m} \approx \frac{\omega_0 e \cos\theta}{m_r x_{n,l}} \approx \frac{ce\cos\theta}{m_r a}. \qquad (3)$$

The precession period can be expressed as $\tau_P = 2\pi/\Omega \approx 2\pi m_r a/ce\cos\theta$. For ethylene glycol at ~600 nm, m_r=1.43. Using the measured values a=1.43 mm and the effective distortion e_{eff}=0.07±0.005, the calculated precession periods are $\tau_A = 1.2\pm0.1$ ns and $\tau_B = 0.7\pm0.1$ ns, which are basically consistent with our measured values. For θ=0°, the calculated value is $\tau_C = 0.6\pm0.1$ ns, which cannot be compared with the experimental result. The reason is that for $\theta = 0°$, $\Delta\phi$ is so large that precession is no longer meaningful.

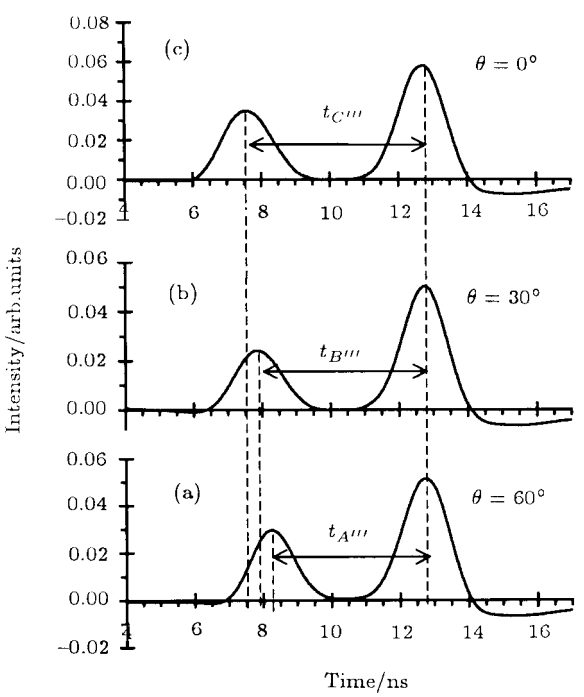


Fig.5. Results of time-resolved measurement. Lasing and the time-delayed reference signals are the left and right pulses, respectively.

Let the vertical dimension of the pendant drop used in our experiment be $2r'_p$, the distortion $e' = (r'_p - r_e)/a$=0.17, a value much larger than the effective distortion and thus leads to a large discrepancy between the calculated and measured precession periods. For the pendant drop used in our experiment, distortion is mainly confined to the top part of the drop, which was in contact with the syringe needle. Other parts of the drop had relatively small distortions. The effective distortion $e_{\mathrm{eff}} = 0.07 \pm 0.005$ deduced from the spectral data for $\theta \leq 65°$ is thus expected to be smaller than e'. Therefore, it is reasonable to use the effective distortion e_{eff} rather than e' to calculate the precession period.

Different lasing patterns are shown in Fig.2 as the pumping position is varied from A to G. At A and B, one pair of lasing spots appears symmetrically at the rim of the pendant drop. At C, two pairs of lasing spots appear near the equatorial plane. When the equatorial plane is illuminated at position D, the two pairs of lasing spots shown in Fig.2(c) merge together. At E, there are two pairs of lasing spots, while only one pair of lasing spots appears when pumping at F and G. The reason that only one pair of lasing spots is observed in Figs.2(A), (B), (F) and (G) is illustrated in Fig.4. As mentioned in the introduction, the trace of a light ray does not form a closed curve after a round trip in a prolate cavity. However, if the distortion is small and the pumping point is at a large enough θ, the trace of one round trip is sufficiently close to the great ellipse that contains the pumping point. We call this kind of trace (one round trip) "great ellipse" (in quote). Note that the shape of the pendant drop is approximately a distorted spheroid with an eccentricity at its upper part larger than that of its lower part. When the pump pulse impinging near the bottom or the top as shown in Figs.2(A), (B), (F) and (G), the lasing radiation circulates along the precessing orbit, the "great ellipse" of which has a larger eccentricity, as depicted in Fig.4(c). The curvature of the "great ellipse" is a maximum at point A'. Majority of the lasing light escapes from that point easily so that only two lasing spots from A' and its axisymmetric position A''' are observed along the $\pm Y$ directions. When the pump pulse impinging near the equatorial plane, the "great ellipse" of its lasing precession orbit has a smaller eccentricity, as depicted in Fig.4(b). The fractions of light leaked out at positions B and B' are comparable, but larger than those at other points of the "great ellipse", so that four lasing spots, namely, B, B' and their axisymmetric points B'', B''' can be observed along the $\pm Y$ directions, as

shown in Figs.2(C) and (E).

It is well known that the Q factor of an asymmetric resonant cavity decreases with the increase of cavity eccentricity.[12] As the eccentricity of a "great ellipse" increases with angle θ, stimulated emission leaks out easier when circulating along a "great ellipse" with larger θ, and the lasing action requires larger pumping energy. Therefore, lasing threshold $E_{\rm th}(\theta)$ increases with angle θ, which is in agreement with our experimental results stated at the end of Section ⅢA.

IV. CONCLUSION

Lasing from the rim of a dye-doped ethylene glycol pendant drop excited by a nitrogen laser was investigated. The lasing wavelength was found to red shift along a vertical rim of the pendant drop. We compared this phenomenon with the theory of splitting of m-mode MDRs and an effective distortion value was deduced for the pendant drop. The lasing was found to precess in the pendant drop by time-resolved measurement. The precession periods for several pumping points were measured, with values consistent with those obtained by a precession formula based on MDR theory. Various lasing patterns caused by lasing precession in the pendant drop were explained.

ACKNOWLEDGMENTS

We would like to thank Profs. K. Young and P. T. Leung for their enlightening discussions. Help of Prof. D. H. L. Ng, Mr. M. K. Lee, Mr. C. W. Chan, Mr. K. K. Lee, and Ms. P. Y. So is gratefully acknowledged.

REFERENCES

[1] A. W. Neumann, R. J. Good, Experimental Methods in Surface and Colloid Science, R. J. Good, R. R. Stromberg, Eds. (Plenum, New York, Vol.11, 1979).

[2] J. A. Lock, *J. Opt. Soc. Am.,* **A10**(1993),693; C. W. Chan, W. K. Lee, *J. Opt. Soc. Am.,* **B13**(1996),532, and the references therein.

[3] S. Chang, N. B. Rex, R. K. Chang, *J. Opt. Soc. Am.,* **B58** (1999),1224.

[4] H.-M. Tzeng, K. F. Wall, M. B. Long, R. K. Chang, *Opt. Lett.,* **9**(1984),499; H.-B. Lin, J. D. Eversole, A. J. Campillo, *J. Opt. Soc. Am.,* **B9**(1992),43.

[5] C. G. B. Garrett, W. Kaiser, W. L. Bond, *Phys. Rev.,* **124**(1961),1804.

[6] T. S. Fahlen, H. C. Bryant, *J. Opt. Soc. Am.,* 58(1968), 304.

[7] S. C. Hill, R. E. Benner, Optical Effects Associated with small particles, P. W. Barber, R. K. Chang, Eds. (World Scientific, Singapore, 1988).

[8] H. M. Lai, P. T. Leung, K. Young, *Phys. Rev.,* **A41** (1990),5187.

[9] P. W. Barber, S. C. Hill, Optical Particle Sizing: Theory and Practice, G. Gouesbet, G. Grehan, Eds. (Plenum, New York, 1988).

[10] G. Chen, R. K. Chang, S. C. Hill, P. W. Barber, *Opt. Lett.,* **16**(1991),1269; G. Chen, M. M. Mazumder, Y. R. Chemla, A. Serpengüzel, R. K. Chang, S. C. Hill, *Opt. Lett.,* **18**(1993),1993.

[11] J. C. Swindal, D. H. Leach, R. K. Chang, K. Young, *Opt. Lett.,* **18**(1993),191.

[12] J. U. Nöckel, A. D. Stone, Optical Processes in Microcavities, R. K. Chang, A. J. Campillo Eds. (World Scientific, Singapore, 1996).